Measured Electromagnetic Shielding Performance of Commonly Used Cables and Connectors

LOTHAR O. HOEFT, MEMBER, IEEE, AND JOSEPH S. HOFSTRA

Abstract—**The intrinsic electromagnetic property of a cable or connector shield is its surface transfer impedance. This is the ratio of the longitudinal open circuit voltage measured on one side of the shield (normally the inside) to the axial current on the other side (normally the outside). In cases where a high electric field is present at the surface of the shield, the transfer admittance or charge transfer elastance is also important. Measurements of typical cables, connectors, backshells, and cable terminations will be presented and explained in terms of simple models.**

Index Code—**F16 b/f.**

I. Introduction

ELECTROMAGNETIC shielding is used to protect electronic equipment and systems from the effects of lightning, nuclear electromagnetic pulse, and electromagnetic interference (EMI). In general, the hostile electromagnetic environment is outside the system, and the electromagnetic shielding is used as a barrier between the hostile environment and the system that must be hardened. Electromagnetic shielding is also used to reduce emanating radiations that could cause electromagnetic compatibility or TEMPEST problems. In this case, the hostile environment is on the inside of the cable and system, and the protected environment is external to the system. In both cases, the shielding acts as a barrier to the electromagnetic radiation. Shielding is added to cables, connectors, and cable assemblies in order to provide this electromagnetic barrier.

Traditionally, some form of shielding effectiveness has been used to specify cable shields and connectors or backshells. The IEEE defines shielding effectiveness as the ratio of the field at a point with and without the shield in place. This has the advantage of being conceptually simple and easy to measure. Unfortunately, there are a number of problems with the concept of shielding effectiveness. The first is that there is a lack of a unique definition. The IEEE definition of shielding effectiveness—the ratio of the field at a point with and without the shield in place—does not fit all situations. In fact, one definition, namely the ratio of the current on the shield to the current on the core wires, has become quite popular. Second, shielding effectiveness is not an intrinsic property of the shields because it depends on the external and internal impedances. This has been pointed out by Madle [1] and others. Thirdly, there is a lack of an independent calibration of shielding effectiveness. There is no standard shield whose shielding effectiveness can be derived from first principles knowing the geometry and material properties. Thus, a shielding effectiveness measurement could be in error due to differences in measurement setup, and the experimenter would not be able to know that he has a measurement problem. In many situations, a particular product can be made to meet specifications simply by varying the reference antenna rather than improving the electromagnetic performance of the product. This is certainly an undesirable situation.

In the 1930's, Schelkunoff showed that surface transfer impedance was the intrinsic shielding property of cables, connectors/backshells, and cable assemblies [2]. Initially, he treated only cylindrical shields. However, his work has been extended to include imperfections in the shield such as apertures, porpoising, etc.

In the early 1960's, Zorzy and Muehlberger [3] used a triaxial test fixture to measure the transfer impedance of connectors at very high frequencies. They reported their results as shielding effectiveness or insertion loss. Their fixture and procedures are the basis for many of the shielding tests performed on connectors such as the MIL-C-39012 and MIL-C-38999. In the 1970's, Knowles and Olsen [4] measured the surface transfer impedance of a number of cable shields. Madle reviewed shielding measurement methods and proposed several test fixtures for measuring surface transfer impedance [1]. During the same time period, Casey and Vance [5], [6] developed and summarized much of the theory of tubular cable shields, with and without apertures. In 1978, Vance provided a comprehensive review of surface transfer impedance theory and application by devoting a chapter to the subject in his book [7] on electromagnetic coupling to shielded cables.

This paper will discuss surface transfer impedance of cables and connectors by first giving the definitions of surface transfer impedance and surface transfer admittance. Then a brief discussion of surface transfer impedance theory will be presented, followed by typical results.

II. Definitions

A. Surface Transfer Impedance

The surface transfer impedance of a cylindrical shield, such as is found on cables, connectors, backshells, and cable assemblies, is defined by the relationship shown in (1); namely, the voltage drop on the inside of the shield divided by the current flowing on the external surface

$$Z_T = \frac{1}{I_0}\frac{dV}{dz}\bigg|_{I=0} \tag{1}$$

Manuscript received March 7, 1988; revised March 28, 1988.
The authors are with the BDM Corporation, Albuquerque, NM 87106.
IEEE Log Number 8821926.

where I_0 is the current flowing on the shield and dV/dz is the voltage per unit length on the inside of the shield. Since surface transfer impedance is an intrinsic property of the shield, the reverse configuration can also be used. The current can be on the inside, and the voltage per unit length can be measured on the exterior surface. In most cases, (1) is simplified to the relationship shown in (2) where V_{oc} is the open circuit voltage on the inside of the shield, I_0 is the current flowing on the shield, and l is the length of the cable sample. Equation (2) is obtained by integrating (1) along the z-axis.

$$Z_T = \frac{V_{oc}}{I_0 l}. \tag{2}$$

B. Surface Transfer Admittance

The complementary coupling quantity is the short-circuit current induced on the center conductor for an electric field on the external surface of the shield. This can be calculated using the surface transfer admittance. Traditionally, this is defined by (3)

$$Y_T = \frac{1}{V_0}\frac{dI_{sc}}{dz}\bigg|_{V=0} \tag{3}$$

where dI_{sc}/dz is the short-circuit current per unit length flowing on the internal conductor of the cable, and V_0 is the voltage between the shield and the external electrode. In most cases, the transfer admittance is related to the transfer capacitance by the relationship shown in (4)

$$Y_T(\omega) = j\omega C_t \tag{4}$$

where the angular frequency ω is equal to $2\pi f$, and C_t is the transfer capacitance (i.e., the capacitance between the external electrode and the center conductor of the cable).

Transfer admittance is important when the electric field at the shield is significant. This is usually not the case since the shield is normally grounded. The electric field will be small as long as the cable is electrically small. Under these conditions, transfer admittance can be neglected. In addition, for cables with high optical coverage, the transfer admittance is so small that its contribution can be neglected. Note that the transfer admittance depends on the external circuit as well as the electromagnetic characteristics of the shield. Thus, it is not an intrinsic shielding property.

Several authors have suggested other parameters, such as charge transfer frequency or charge transfer elastance for characterizing electric field coupling through cable shields [8], [9]. The charge transfer elastance or S_s parameter is the ratio of the transfer capacitance to the internal and external capacitances. This is generally an intrinsic property of the shield. Unfortunately, measurements of transfer admittance are seldom reported. Reference [10] presents one of the few laboratory measurements of surface transfer admittance reported in the literature.

III. Theory

A. Tubular Shields-Diffusion Coupling

For a thin, tubular shield, only current diffusion is important. In this case, the surface transfer impedance is given by (5) [7]

$$Z_T = R_0 \frac{(1+j)T/\delta}{\text{Sinh}\,(1+j)T/\delta} \tag{5}$$

where T is the wall thickness and δ is the skin depth. The dc resistance of the shield R_0 is given by the following equation:

$$R_0 = \frac{1}{2\pi a \sigma T} \tag{6}$$

where a is the radius of a cylindrical shield and σ is the conductivity of the shield material. The skin depth δ is the distance that the current can diffuse into the shield material during each cycle. The skin depth can be calculated using (7)

$$\delta = \frac{1}{\sqrt{\pi f \mu \sigma}} \tag{7}$$

where f is the frequency and μ is the permeability of the shield material which is equal to $4\pi \times 10^{-7}\ \mu_r$. Note that the skin depth is frequency dependent, varying inversely with the square root of the frequency. Another way to characterize current diffusion is to define the diffusion time constant, which is the time it takes the current to diffuse from the outer surface of a cylindrical shield to the inner surface. The diffusion time constant is given in (8)

$$\tau_\delta = \mu \sigma T^2. \tag{8}$$

When analyzing surface transfer impedance in the frequency domain, the current diffusion break frequency is often a useful way of characterizing this type of coupling. The current diffusion break frequency f_δ is the frequency where the skin depth is equal to the thickness of the shield. Its relationship to the quantities discussed earlier is given in (9)

$$f_\delta = \frac{1}{\pi \tau_\delta} = \frac{1}{\pi \sigma \mu T^2}. \tag{9}$$

The surface transfer impedance of a cylindrical shield, such as described by (5), has been calculated by Vance [7] and is shown in Fig. 1. The surface transfer impedance is normalized by dividing by its dc resistance. For frequencies up to the break frequency, the surface transfer impedance is equal to the cable's dc resistance. Above the current diffusion break frequency, the surface transfer impedance drops rapidly, indicating that the current no longer diffuses through the shield, and the shield is acting more and more like an impervious electromagnetic barrier. The preceding discussion pertains primarily to cylindrical shields. For shields of other geometries, such as rectangular shields or shields of arbitrary cross section, the physical principles presented in the preceding discussion are still valid. However, the equations for calculating the sample's dc resistance would change. The dc resistance can usually be calculated by considering the shield as a piece of metal wrapped around the cable core, and the dc resistance of such a piece of metal is the length divided by the product of the cross-sectional area and the conductivity.

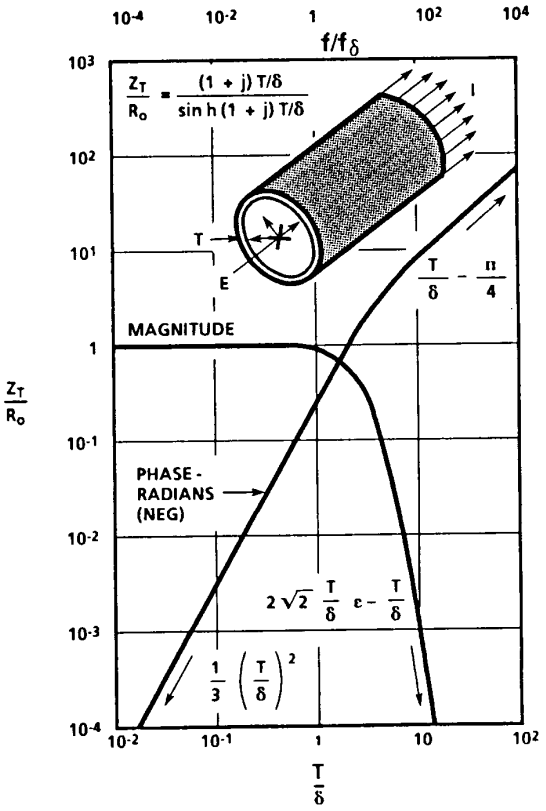

Fig. 1. Surface transfer impedance of a cylindrical shield.

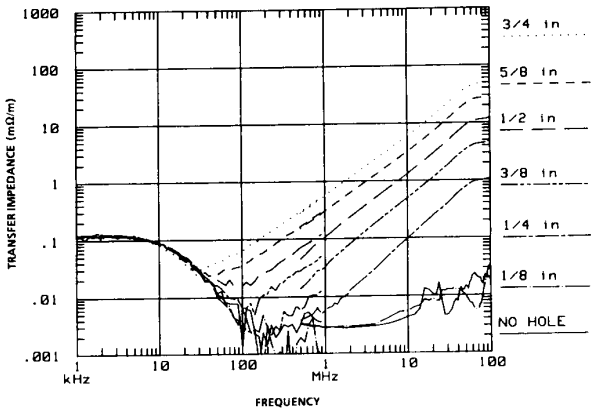

Fig. 2. Surface transfer impedance of a shield with imperfections.

B. Imperfect Shields, Aperture and Porpoising Coupling

If the shield has imperfections like apertures or penetrations (for example, the carriers of a braided shield), (5) must be modified to account for the coupling due to the imperfections. These imperfections are modeled as a mutual inductance. Thus, (5) can be rewritten by adding a mutual inductance term. The surface transfer impedance then becomes

$$Z_T = R_0 \frac{(1+j)T/\delta}{\text{Sinh}\,(1+j)T/\delta} + j\omega M_{12} \tag{10}$$

where ω is the angular frequency and M_{12} is the shield mutual inductance. A braided shield may have a mutual inductance due to both apertures and porpoising.

Apertures are formed by the intersections of the carriers. If the braid does not completely cover the exterior of the shield and the optical coverage is less than 100 percent, the braid will have small diamond-shaped apertures at the intersections of the carriers.

Porpoising coupling occurs because of the finite contact resistance or impedance between the carriers as they pass from the outside to the inside of the cable shield [11], [12]. When the carrier is on the outside of the cable, it carries the external shield current. Because of the finite impedance between the carriers, some of this current remains on the carrier as it reaches the inside of the cable shield. Porpoising coupling is characterized by a surface transfer impedance that increases at 10 dB per decade in the vicinity of 1 MHz and eventually behaves as a mutual inductance. Note that the imperfections, such as aperture and porpoising coupling, are both high-frequency effects; they cause the surface transfer impedance to increase with frequency. These imperfections are usually important only above 1 MHz.

Aperture coupling depends on the magnetic polarizability of the apertures. The mutual inductance of an aperture [13] can be predicted using (11)

$$M_{12} = \frac{\mu_0 \alpha_m}{(\pi D)^2} \tag{11}$$

where α_m is the magnetic polarizability. The mutual inductance of a complete cable is the mutual inductance of a single aperture multiplied by the number of apertures. The magnetic polarizability for a circular hole [14] or rectangular slot is shown in (12) and (13), respectively

$$\alpha_m = \frac{4}{3} r^3 \text{ (Circular Hole)} \tag{12}$$

$$\alpha_m = \frac{\pi}{16} W^2 l \text{ (Rectangular Hole).} \tag{13}$$

In certain cases where the apertures are significant, such as in a calibration pipe that may have rather large holes, the electric field contribution can be included through the use of an effective magnetic polarizability [15]. This is shown in (14)

$$\alpha_{m_{\text{eff}}} = \left(1 + \frac{\alpha_e}{\alpha_m}\right) \alpha_m. \tag{14}$$

In general, the electric polarizability (α_e) is equal to one-half the magnetic polarizability. Fig. 2 shows a typical transfer impedance measurement of a shield with an aperture. This particular sample is a 32-mm (1-1/4 in) diameter copper pipe with a single hole of various diameters. A similar frequency dependence would be expected of a braided cable where the high-frequency coupling was dominated by porpoising coupling.

There are no simple relationships for calculating porpois-

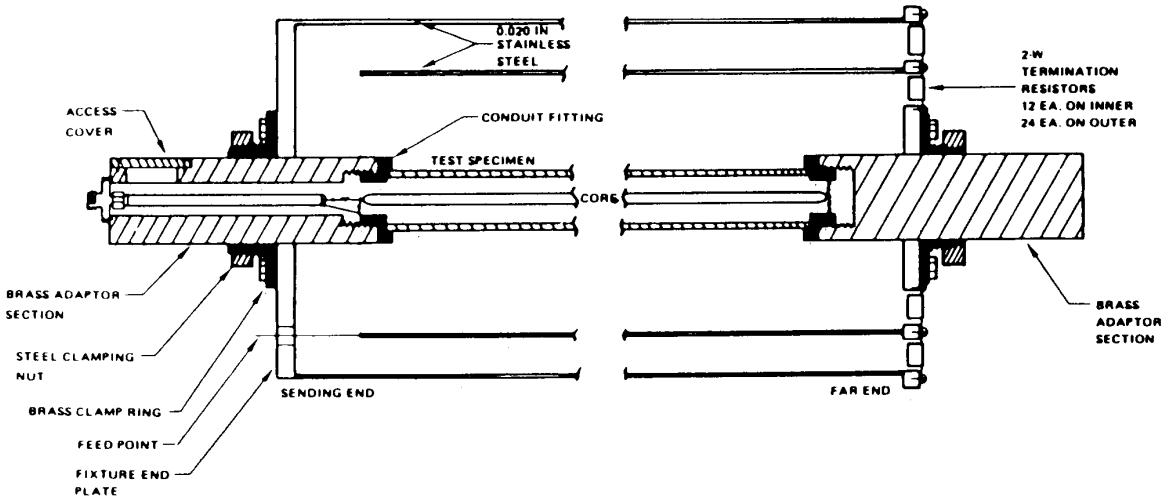

Fig. 3. Schematic diagram of the quadraxial test fixture used for cable transfer impedance measurements.

ing coupling. In general, however, porpoising coupling is opposite in phase compared to aperture coupling. Thus, aperture coupling can be balanced against porpoising coupling to give an optimized braid. The high-frequency performance of most cables is determined by porpoising coupling because it is evidence of more than optimum braid, and most cable designers tend to err on the side of too much optical coverage rather than too little.

IV. Measurement Techniques

Surface transfer impedance may be measured using a variety of techniques. In general, the more sophisticated the test fixture, the broader its bandwidth, and the easier it is to use. A review of surface transfer impedance measurement methods is given in [8].

Almost all of the data presented in this paper were taken using a quadraxial test fixture and a computer controlled data acquisition system. In a quadraxial test fixture, the shield under test becomes the center conductor of a terminated transmission line. Another terminated transmission line is formed by the guard or outer electrode placed around the drive line. Since all the transmission lines are terminated, standing waves are eliminated and a broad-band test fixture results. Fig. 3 shows a cross-sectional view of the quadraxial test fixture used to make the most of the cable measurements in this paper, and Fig. 4 shows a cross-sectional view of the quadraxial test fixture used for the connector and backshell measurements. Since the drive line is a terminated transmission line, the shield current can be obtained by measuring the voltage on this line. The voltage divider resistor in the test fixture isolates the 50-Ω input impedance of the reference channel from the drive circuitry, in addition to reducing the signal to an appropriate range for the network analyzers.

Most of the measurements presented here were taken with the computer controlled data acquisition system shown in Fig. 5. Two network analyzers were necessary to cover the frequency range from 5 Hz to several hundred MHz. These network analyzers were under the control of a microcomputer via the IEEE 488 instrumentation bus. Signal amplifiers and power amplifiers were used to adjust the signals and optimize the dynamic range of the measurement system. In addition to the ac instruments shown in Fig. 5, the dc resistance of every sample was measured by passing 10 A through the shield and measuring the voltage drop. Comparison between the dc resistance and the ac transfer impedance at low frequencies provided an important check of the validity of the measurements. The two measurements generally agreed to within 10 percent (1 dB).

The test fixtures were checked out using calibration samples, i.e., samples, such as solid pipes with and without defined holes, whose surface transfer impedance could be predicted from first principles. Fig. 6 shows the measured and predicted transfer impedance of the calibration standard used for the cable measurements. This standard was a 15.9-mm (5/8-in) diameter brass calibration shield 1 m long and had a dc resistance of 1 mΩ. Besides establishing the credibility of the measurements up to a frequency of 1 MHz, the use of this calibration sample establishes the noise floor of the measurement system. This was slightly over 1 μΩ/m in the measurement shown in Fig. 6. A second calibration shield, identical to the first except for the presence of 22, 3.18-mm (1/8-in) diameter holes, was used to check the high-frequency response. Fig. 7 shows a typical measurement. At low frequencies, the response of the two calibration samples was similar and is indicative of diffusion coupling through a solid pipe. Above 400 kHz, aperture coupling dominated, and the measured surface transfer impedance increased at the rate of 20 dB/decade as predicted by theory. Around 100 MHz, the sample was no longer electrically short and transfer impedance was no longer being measured. Rather, a voltage response related to the long line response of a cable was being measured. In some of the early measurements presented in this paper, computations were used to correct the measurements for this effect. Such calculations were difficult to apply and not too successful. Fig. 8 shows the calibration measurements for the connector test fixture. The calibration samples were 15.9-

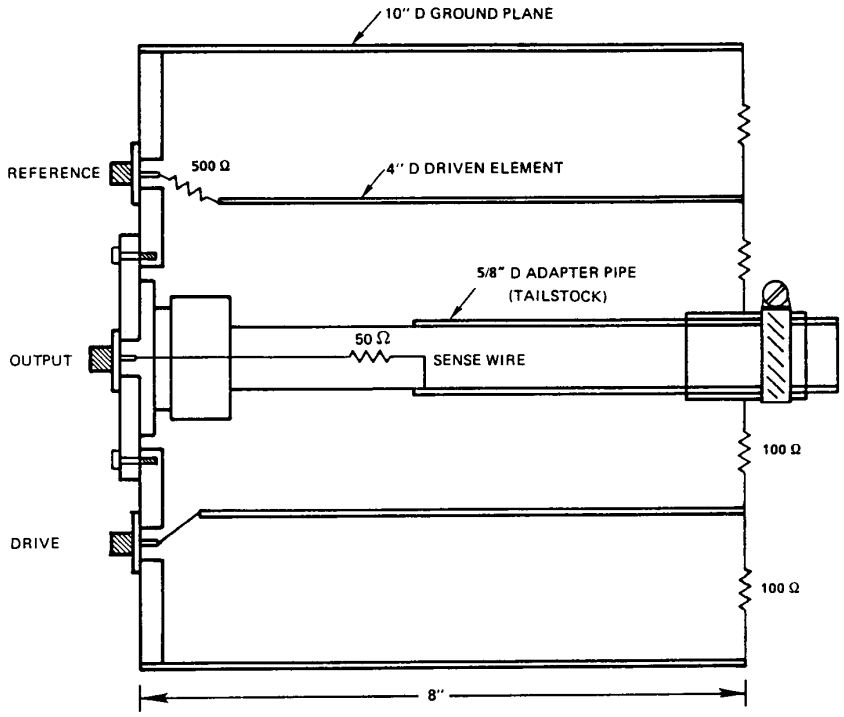

Fig. 4. Schematic diagram of the quadraxial test fixture used for measuring the surface transfer impedance of connectors and backshells.

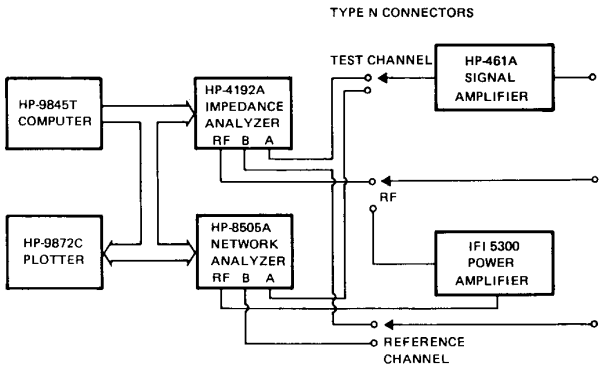

Fig. 5. Computer controlled data acquisition system.

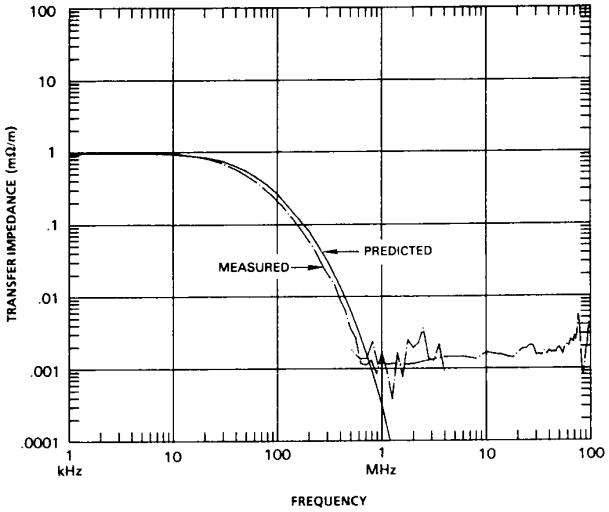

Fig. 6. Measured surface transfer impedance of a 16-mm (5/8-in) diameter brass calibration shield (dc resistance is 1 mΩ/m).

mm (5/8-in) diameter copper pipes, one of which had a single 3.8-mm (0.15-in) diameter hole. Since the fixture was smaller, transfer impedance could be measured to a higher frequency.

V. Typical Results

A. Tubular Shields without Imperfections

Tubular shields without imperfections, such as rigid electrical conduit or water pipe, can be extremely cost-effective cable shields for electromagnetically hardened ground facilities, if they are installed correctly. The surface transfer impedance of solid walled nonferromagnetic cable shields, such as copper water pipe, can be accurately predicted using (5). A 22-mm (7/8-in) diameter copper pipe with a wall thickness of 1.6-mm (1/16-in) has a dc resistance of less than 1 mΩ/m and a diffusion break frequency of less than 10 kHz. A corresponding rigid thin-walled steel conduit has a slightly higher dc resistance (a few milliohms per meter) but much lower diffusion break frequency (a few hundred hertz) [17]. Black iron water pipe (33-mm diameter, 3.34-mm wall thickness) has a lower dc resistance and diffusion break frequency because of the increased wall thickness. Recent measurements [17] show that the relative permeability of steel and iron is frequency independent, at least for frequencies

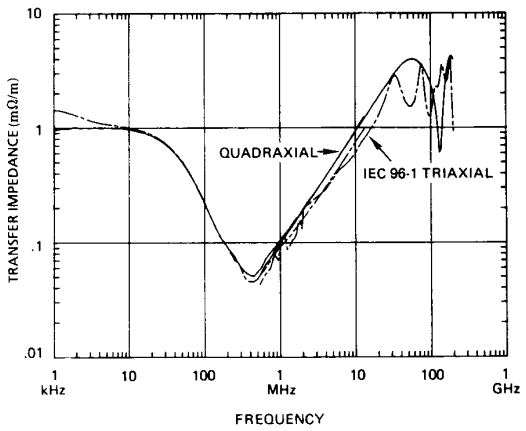

Fig. 7. Measured surface transfer impedance of a brass calibration pipe with 22 3.175-mm (1/8-in) diameter holes.

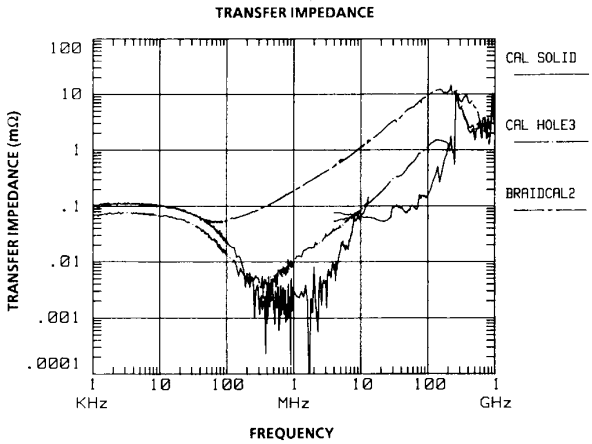

Fig. 8. Measured surface transfer impedance of the calibration shield used in conjunction with the connector test fixture.

below 1 MHz. Above 1 MHz, the surface transfer impedance is so small that the frequency dependence of the relative permeability is immaterial. When relatively new, the compression joint fittings used to join sections of thin-walled steel conduit displayed a very low transfer impedance, being equivalent to a very short section of conduit [17]. The surface transfer impedance of joint fittings using set screws increased as the square root of frequency, suggesting that its performance was limited by contact impedance. Above 1 kHz, the set screw fitting was significantly worse than the compression fitting. Both could be expected to degrade with time. Welded, soldered, brazed, or threaded joints should be more stable.

B. Braided Shields

Fig. 9 shows a typical measurement of the surface transfer impedance of a 1-m-long tin-plated, copper braided shield. This figure shows the measured transfer impedance for single, double, and triple overbraids [18]. At low frequencies, the surface transfer impedance, which was really the transfer resistance, was inversely proportional to the number of shields. At high frequencies (above 0.5 MHz), the surface transfer impedance decreased about an order of magnitude (20 dB) as each shield was added. Careful examination of the region between 500 kHz and 5 MHz shows that the transfer impedance of the single braid was increasing at the rate of 10 dB per decade rather than the expected 20 dB per decade. This indicates that the primary coupling mechanism was porpoising coupling, at least for the single tubular braid sample in this set of measurements. A model for predicting the transfer resistance and mutual inductance of braided cable shields using jacket diameter as the independent parameter [19] will be presented later in this paper.

C. Flexible Conduits

Fig. 10 shows the measured transfer impedance of three flexible metal core conduit assemblies showing the effect of added tinned copper braid [20]. The measurement labeled "Bronze Overbraid No. 1" was a brass metal core conduit with bronze overbraid. It was typical of a thin, solid cylindrical shield made of relatively low conductivity brass and bronze overbraid. Its surface transfer impedance was not particularly good. The addition of a tinned copper overbraid (sample 4) decreased the high-frequency transfer impedance so much that it was below the noise level of the system for frequencies above 1 MHz. Fig. 11 shows the comparison between brass convolute samples covered with both a tinned copper braid and with either a SnCuFe (tinned copper-plated iron) or tinned copper braid [20]. Notice that the higher permeability of the SnCuFe braid is evident in the measured transfer impedance between about 10 and several hundred kHz. Above 1 MHz, the transfer impedance of the shield was below the measurement capability of the system. SnCuFe has a lower conductivity than tinned copper. This is evident in the higher surface transfer impedance of the SnCuFe sample below 5 kHz.

Fig. 12 shows the measured transfer impedance of samples that incorporated ferromagnetic conduits [18]. Sample 58, a molypermalloy annular hose, did not have an overbraid, and therefore had a rather high (60 mΩ/m) transfer resistance. However, it had essentially negligible surface transfer impedance above a couple of MHz. In Sample 15, the high permeability convolute had a current diffusion break frequency below 1 kHz. Therefore, a comparison between the measured surface transfer impedance and its dc resistance could not be made. Sample 48, which used mu-metal tape between two layers of nickel-plated copper overbraid, was one of the lowest transfer impedances measured at our laboratory.

Most of the flexible conduits described in the preceding paragraphs were manufactured by forming a spiral strip of metal and soldering the assembly together so that it forms a solid conduit without apertures. The solder ensured that the impedance between the turns of the spiral was very low. Nonsoldered spiral conduit is sometimes used where mechanical protection is the primary design requirement. Figs. 13 and 14 show the measured transfer impedance of such conduit made of aluminum and stainless steel, with and without an overbraid [18]. Without an overbraid, these conduits had very

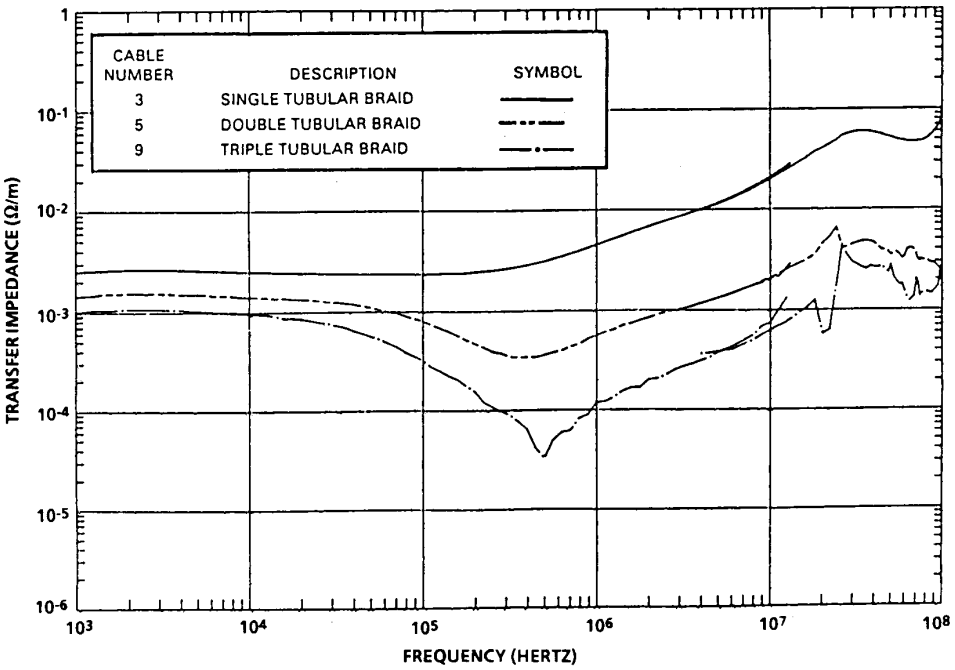

Fig. 9. Measured surface transfer impedance of 1-M long, tin-plated copper, tubular-braided shields.

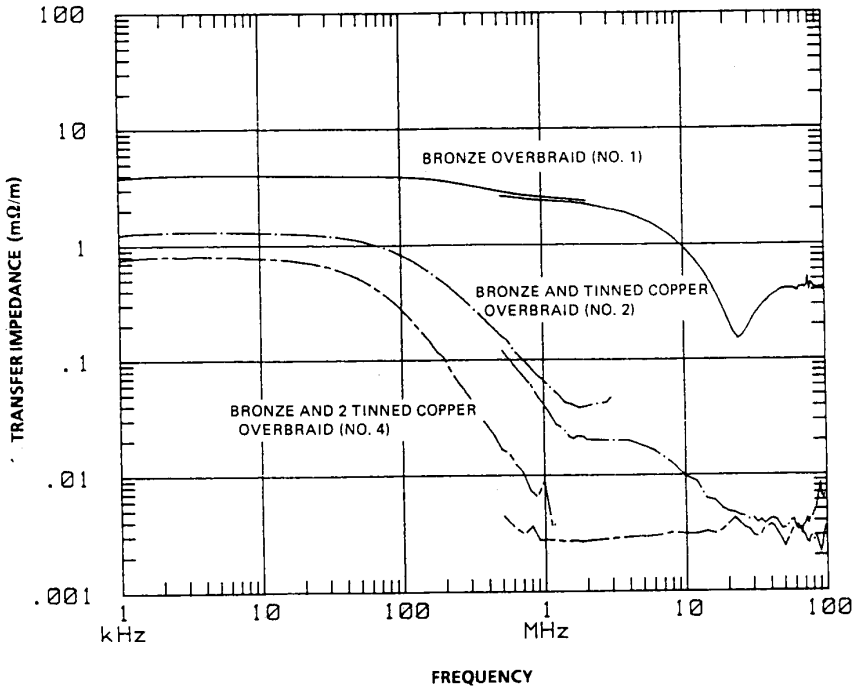

Fig. 10. Measured transfer impedance of three flexible metal-core conduit assemblies showing the effect of adding tinned copper braids.

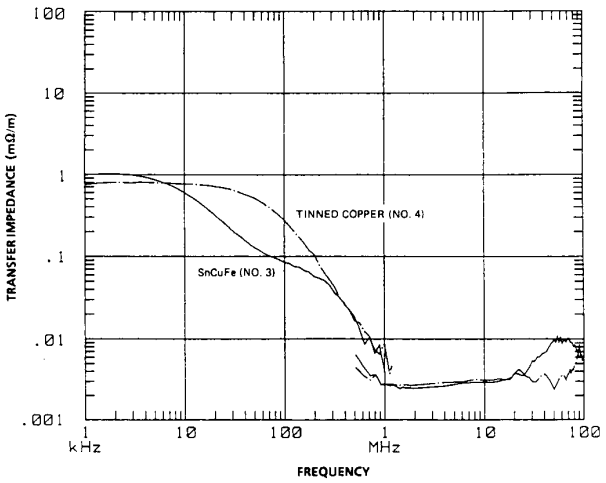

Fig. 11. Comparison of flexible metal-core conduit assemblies with Sn-CuFe or tinned copper as the middle braid.

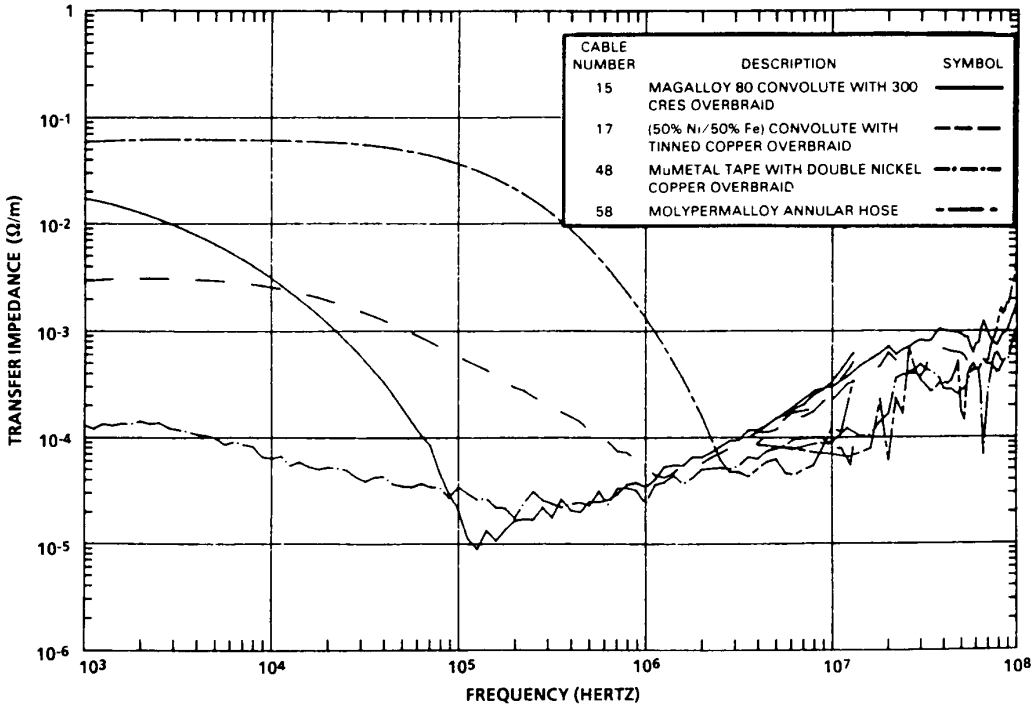

Fig. 12. Measured surface transfer impedance of 1-m long flexible metal-core conduits made of ferromagnetic materials.

high transfer impedances because there was little turn-to-turn contact. They could be modeled as a long strip of metal wound into a solenoid. The result was a high transfer resistance and a high transfer mutual inductance. Adding an overbraid reduces the transfer impedance by orders of magnitude.

D. Metallized Tape and Wire Mesh

In some cases, a shield must be placed over an existing cable or the cable harness is so complicated that a normal machine braid would be too expensive. Metalized plastic tape or knitted wire mesh is sometimes suggested for these applications if the shielding requirements are not too stringent. Figs. 15–17 show the measured transfer impedance of these types of cable shields [21]. The transfer impedance of circumferentially wound metalized plastic tapes, such as those shown in Fig. 15, was very high and showed no evidence of turn-to-turn contact. Fig. 16 compares the performance of circumferentially and longitudinally applied copper-coated plastic tape. The surface transfer impedance of longitudinally applied tape (cigarette wrap) was surprisingly good (10–15 mΩ/m). Fig. 17 shows that the surface transfer impedance of knitted wire mesh was a few tens of mΩ/m and was frequency independent.

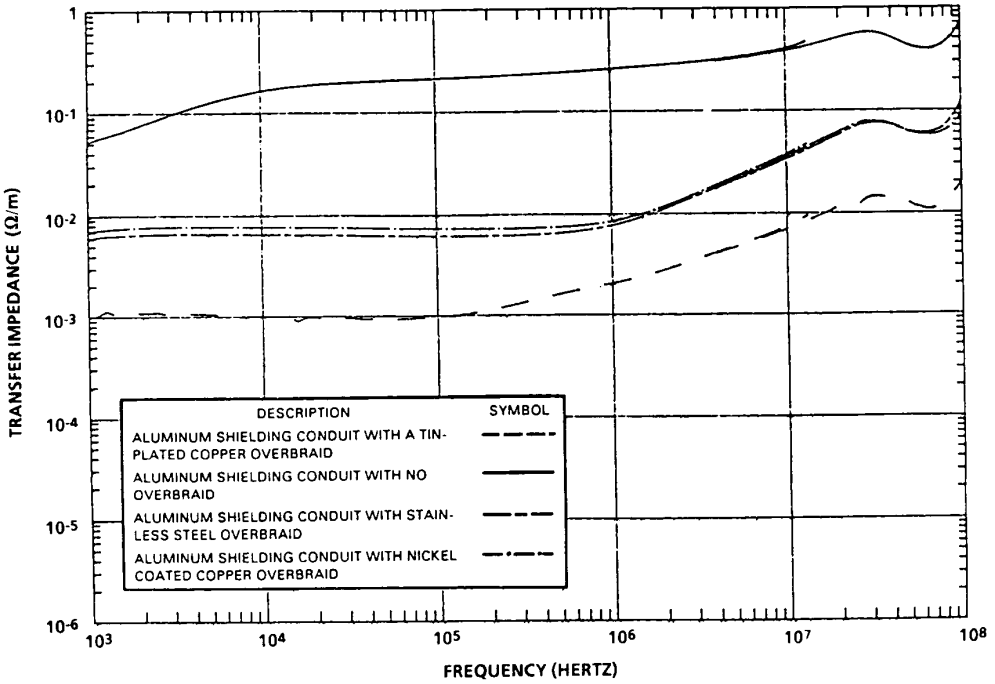

Fig. 13. Comparison of the measured surface transfer impedance of a flexible aluminum shielding conduit, illustrating the effects of different overbraid materials.

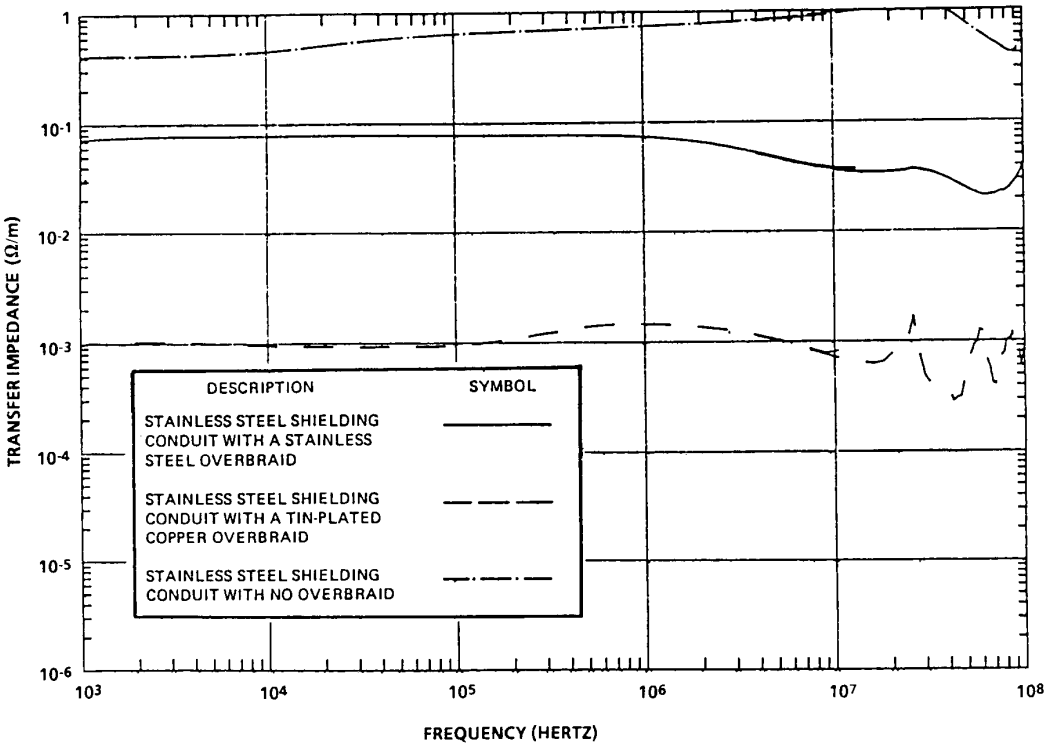

Fig. 14. Comparison of the measured surface transfer impedance of a flexible stainless steel conduit showing the effects of different overbraid materials.

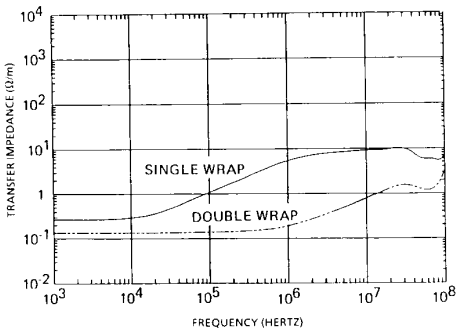

Fig. 15. Measured surface transfer impedance of single and double wrap cable shields constructed using double sided aluminized polyester tape.

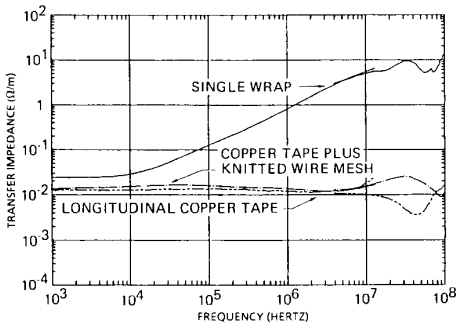

Fig. 16. Measured surface transfer impedance of cable samples that used longitudinally applied copper coated polyester tape and a combination of circumferentially wound copper coated polyester tape and knitted wire mesh.

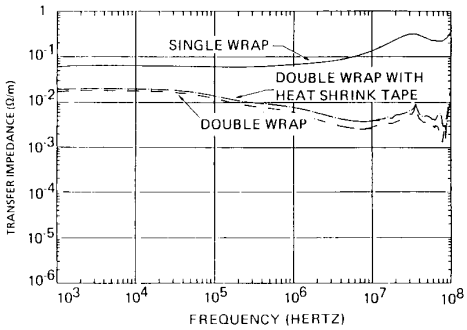

Fig. 17. Measured surface transfer impedance of single and double wrapped cable shield constructed using knitted wire mesh.

E. Connectors, Backshells, and Braid Termination

A shielded cable assembly, such as is used to protect a system from the effects of EMP and EMI, consists of shielded cable, connectors, and backshells. From an electromagnetic shielding point of view, the backshell is an accessory that connects the barrel of the connector to the shield of the cable. The interface between the connector and the backshell is usually threaded and constructed in accordance with the appropriate military standard. The interface between the backshell and the cable shield, usually braid, can take on many different forms, being limited only by the imagination of the backshell designer for producing a product that has good

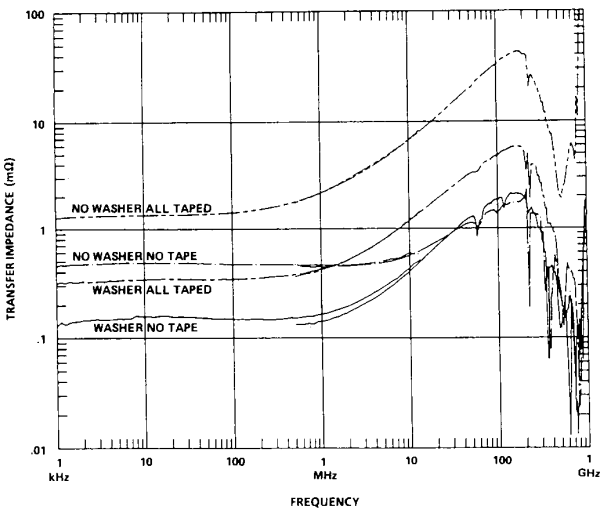

Fig. 18. Measured surface transfer impedance of a MIL-C-38999-500 connector pair with backshell and short length of braid, showing effect of wavy washer and spring fingers.

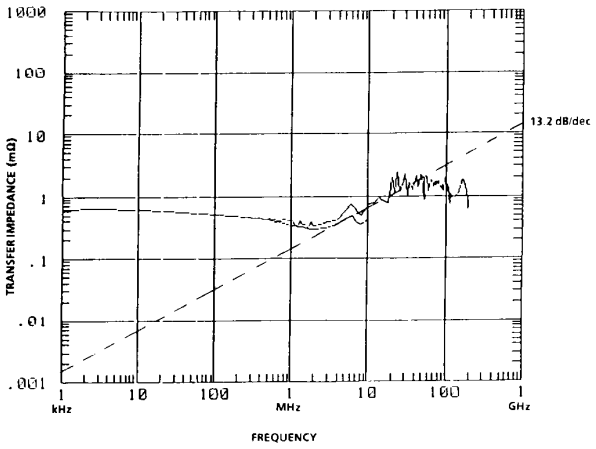

Fig. 19. Typical measurement of a MIL-C-38999 connector pair with backshell and electromagnetically formed braid termination.

electromagnetic characteristics, is easy to use, maintains its integrity during its lifetime, and is economical to manufacture. Typical designs for the backshell–braid interface include a variety of dual cones, a large screw thread, a circular coil spring, metal bands, and various permanent assembly techniques such as a swaged ring, solder, and an electromagnetically compressed ring.

Fig. 18 shows the surface transfer impedance of a typical modern connector (MIL-C-38999, Series IV-500) with an RFI/EMI backshell and a short length of braid measured using a quadraxial test fixture [22]. The backshell used a large screw thread or "lightbulb" to attach the braid. In this case, the connector was degraded in various ways such as removing the wavy washer or taping over the spring fingers. The resulting changes in the surface transfer impedance were clearly evident.

Fig. 19 shows the surface transfer impedance of a connec-

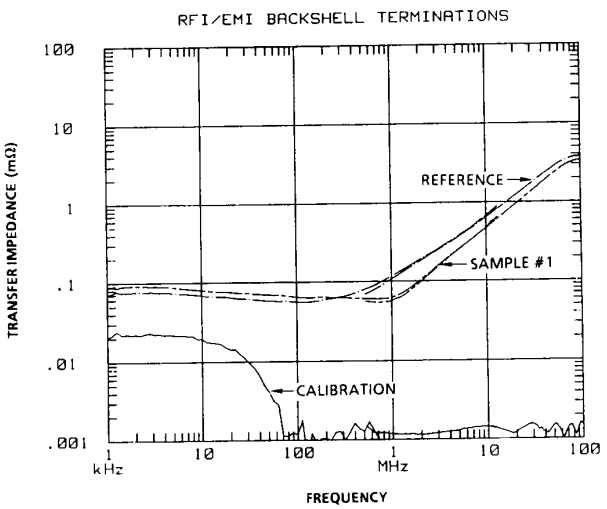

Fig. 20. Measured surface transfer impedance of the instrument calibration, reference, and swaged braid samples.

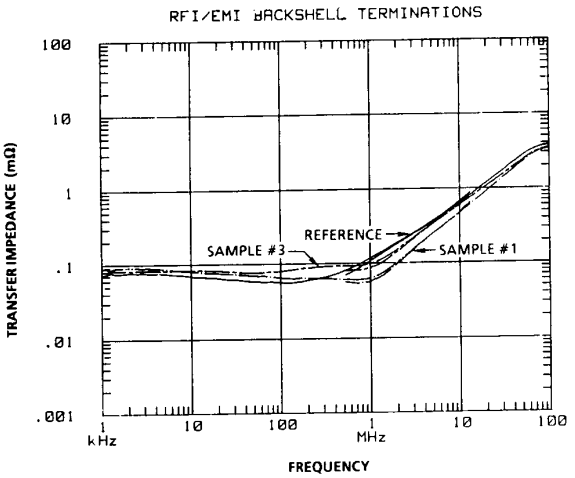

Fig. 21. Measured surface transfer impedance of the reference sample, the swaged braid sample (#1), and a typical dual cone RFI/EMI backshell termination (#3).

tor/backshell/shield termination measured using an inside-out triaxial test fixture [23]. This connector was one of 22 that were measured in a test series. The mean transfer resistance of the series of measurements was 0.7 mΩ with a standard deviation of 0.3 mΩ. The mean surface transfer impedance at 20 MHz was 1.1 mΩ with a standard deviation of 0.5 mΩ. Note that the transfer impedance shown in Fig. 16 does not increase at 20 dB/decade, as would be expected of a shield with an aperture. Instead, the transfer impedance increases at 13 dB/decade, which is closer to the 10 dB/decade expected from coupling due to contact impedance. The mean slope for this set of connectors/backshells/cable terminations was 14 dB/decade with a standard deviation of 5 dB/decade. This suggests that the electromagnetic performance was limited by contact impedance rather than apertures.

In order to determine the major contributions of each part of a shielded connector/backshells/braid termination assembly, special samples were prepared that incorporated only a part of the overall assembly [23]. A solid copper pipe was used as a calibration sample. A 25-mm (1-in) length of single tinned copper braid soldered to the solid portion of the pipe and flange used to attach the sample to the test fixture was a reference sample. The other samples used a variety of techniques to attach the 25-mm length of braid to the backshell. Dual cones were used in five samples. Additional samples used a large screw thread or "lightbulb," a circular coil spring compressed between two cones, and a swaged fitting.

Fig. 20 shows the measured surface transfer impedance of the calibration sample (a solid pipe), the reference sample (25 mm of braid soldered to the solid portion of the sample), and sample 1 (25 mm of braid soldered to the copper pipe and swaged to the nickel-plated aluminum flange section of the sample). These data show that the reference sample had a transfer resistance of a little less than 0.1 mΩ and a transfer inductance (high-frequency transfer impedance divided by the angular frequency ($2\pi f$)) of about 10 pH.

A typical (not worst case) braid, 25 mm in diameter, has a transfer resistance of about 4 mΩ/m and a transfer mutual inductance of between 400 to 800 pH/m [19]. Thus, 25 mm of single braid would be expected to have a transfer impedance that is very close to these measurements. There was very little difference between sample 1 and the reference sample.

Fig. 21 shows the measured transfer impedance of the reference sample (soldered braid), sample 1 (swaged braid), and sample 3 (a typical RFI/EMI backshell that uses clamping cones). There is no significant difference among these three samples.

The remaining four samples that used dual cones to attach the braid gave similar results except that small changes in the tension or position of the sample changed the high-frequency transfer impedance by at least an order of magnitude because changes in the contributions of the braid apertures and porpoising (which depend on contact impedance and therefore braid tension) resulted in large changes in the transfer mutual inductance. Fig. 22 shows an example of the changes that resulted from small changes in the position or tension of the braided shield [23].

Figs. 23 and 24 show the measured surface transfer impedance of samples that used a large screw thread or "lightbulb" and a circular coil spring between cones to make the braid attachment. Several measurements were made of each sample. The variability in the mutual inductance, discussed previously, is clearly evident. The sample that used a circular coil spring between two cones to attach the braid also showed variability in the transfer resistance. This may have been due to variations in the assembly torque, which was not controlled for these measurements.

Recent measurements of backshells that use metal bands for attaching the braid confirms that the braid dominates the electromagnetic coupling above a few megahertz. The transfer resistance of the banded backshell-braid interface was approximately equal to the braid's dc resistance (100 $\mu\Omega$).

A second set of special samples were obtained that

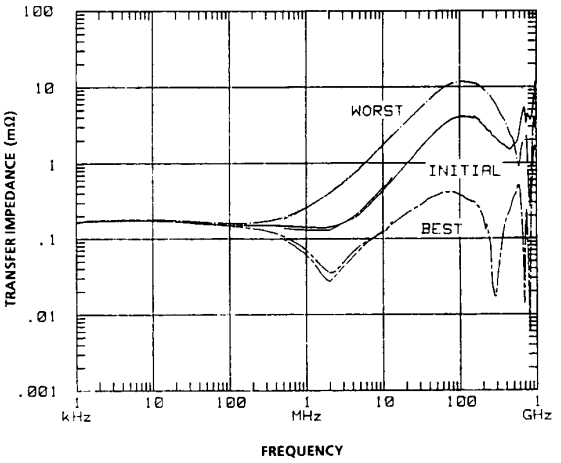

Fig. 22. Several measurements of the surface transfer impedance of a dual cone RFI/EMI backshell termination, before and after braid tension was changed.

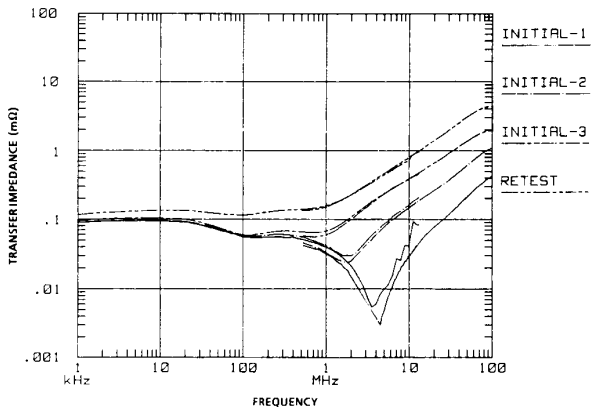

Fig. 23. Measured surface transfer impedance of an RFI/EMI backshell termination that used a large screw thread to attach the shield braid.

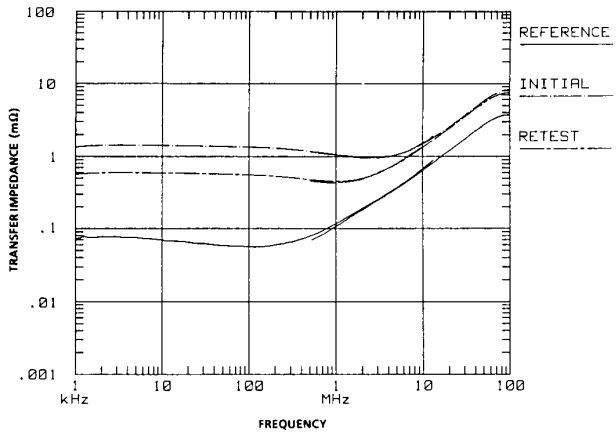

Fig. 24. Measured surface transfer impedance of an RFI/EMI backshell termination that used a circular coil spring to attach the shield braid.

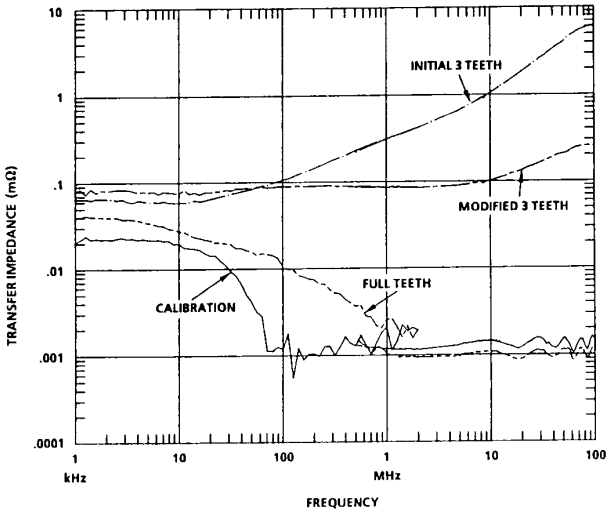

Fig. 25. Measured surface transfer impedance of samples using the MS 3155 connector/backshell interface.

incorporated only the threaded connector–backshell interface appropriate for a wide range of military specifications [24].

Fig. 25 shows the measured transfer impedance of the instrument calibration sample (a solid pipe) and two variations of the MS3155 connector–backshell interface. One of these samples had three clocking teeth and one had a full set of such teeth. Two measurements of the three tooth sample are shown in Fig. 25. In the initial measurement, the surface transfer impedance was proportional to frequency above 1 MHz. This frequency dependence is indicative of aperture coupling. Examination of the test sample revealed that the teeth on the "connector" were wider than the mating teeth on the "backshell." This mechanical mismatch resulted in a gap between the two parts of the sample. After the "connector" teeth were machined so that they fit in the "backshell," the surface transfer impedance was reduced by over an order of magnitude. Between 10 and 100 MHz, the transfer impedance of the modified sample still increases but is proportional to the square root of frequency. This suggests that the coupling mechanism is contact impedance rather than aperture coupling. The surface transfer impedance of the MS3155 sample with a complete set of clocking teeth decreased with frequency up to about 1 MHz. Above 1 MHz, the transfer impedance was below the noise level of the system. These measurements suggest that the sample with full teeth is almost as good as a solid cylindrical shield.

Surface transfer impedance measurement of samples using MIL-C-28840, MIL-C-81511, MIL-C-26482 (Series I), DIN29729, and MIL-C-38999 (Series I/II) interfaces gave similar results. A sample using the MIL-C-38999 (Series III/IV) interface gave higher than expected results. Therefore, a test series that explored the effect of torque was undertaken. After the threads were lubricated, the sample was assembled while controlling the torque. The results are shown in Fig. 26. At 25 in-lbs, the transfer impedance was almost frequency independent. As the torque was increased, the surface transfer impedance decreased. This was particularly evident at the high

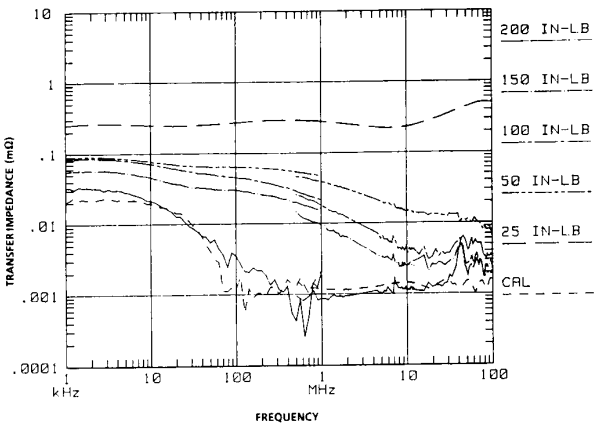

Fig. 26. Effect of torque on the surface transfer impedance of a sample using the MIL-C-38999, series III/IV connector backshell interface.

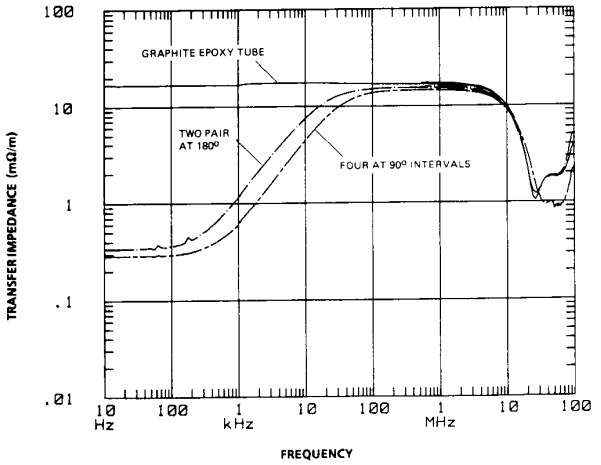

Fig. 27. Measured surface transfer impedance of a large graphite epoxy tube with and without current diverters.

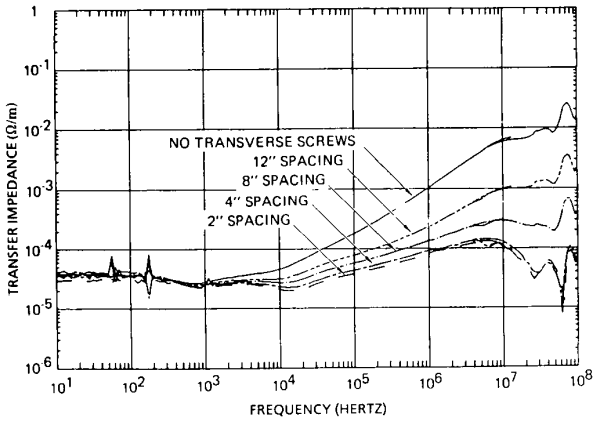

Fig. 28. Measured surface transfer impedance of a large cableway showing the effect of transverse screw spacing.

frequencies. At 200 in-lbs, the transfer impedance of the sample that used the MIL-C-38999, Series III/IV interface approached that of the sample that used the Series I/II interface. Thus, the initial measurement of the sample that used a MIL-C-38999, Series III/IV interface was anomalously high because a lack of lubrication prevented the assembly from coming together properly.

Comparison of the surface transfer impedance of the connector–backshell and backshell–braid interfaces with the surface transfer impedance of a complete connector assembly (Figs. 18 and 19) shows that 25 mm of single braid will dominate the coupling at high frequencies. That is, the surface transfer mutual inductance of this short length of braid (10–30 pH) is higher than the impedance attributed to any of the backshell to braid termination methods or any of the connector to backshell interfaces (properly assembled). Of course, the statement is true only for the braid termination techniques that provide low inductance (essentially 360°) contact between the braid and backshell. Pigtail terminations would normally have mutual inductances two to four orders of magnitude worse than an inch of braid. The resistance of 25 mm of braid (0.1 mΩ) was comparable to the resistance of the backshell–braid interface and was comparable or slightly less than the connector–backshell interface (properly torqued). These three interfaces can account for several hundred microohms of a complete assembly. The connector and backshell barrels have a resistance of a few tens of microohms; therefore, the spring fingers that form the joint between the connector plug and receptacle must have a resistance of 300–600 μΩ. Aperture coupling in the connector appeared to be insignificant compared to the coupling through the braid.

In operational systems, the most common cable assembly degradation is the loosening of the backshells or improper reassembly of the connector–backshell–braid interface. These degradations can increase the transfer impedance of a cable assembly by orders of magnitude.

F. Other Shields

Surface transfer impedance measurements are not limited to cables and connectors. They can also be used to characterize any type of shield that is longer than it is wide. Fig. 27 shows the measured transfer impedance of a 0.3-m-diameter graphite epoxy tube in which four copper current diverters were added to its sides [25]. The difference between resistive and inductive current division is clearly evident. Fig. 28 shows the measured transfer impedance of a 0.2 × 0.6 m aluminum cableway in which the transverse screw spacing was varied [26]. Measurements such as those shown in Fig. 28 can be used to guide the design of such cableways so that they provide sufficient shielding and are economical to produce.

G. Models for Predicting Surface Transfer Impedance

Frequently, one wants to predict the surface transfer impedance of cables in order to design a cable or to predict the response of a cable shield in a hostile environment. The theory presented in the previous section can be used to provide a theoretical foundation for a surface transfer impedance prediction model. The surface transfer impedance is usually divided into a transfer resistance and a transfer mutual inductance (see (10)). As stated in the theory section, to a first approximation, the transfer resistance is determined by the amount of metal in

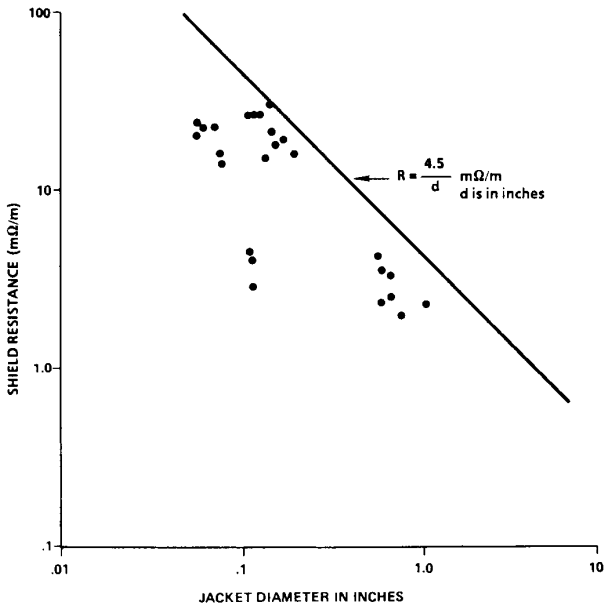

Fig. 29. Shield resistance as a function of cable diameter of single braid cables.

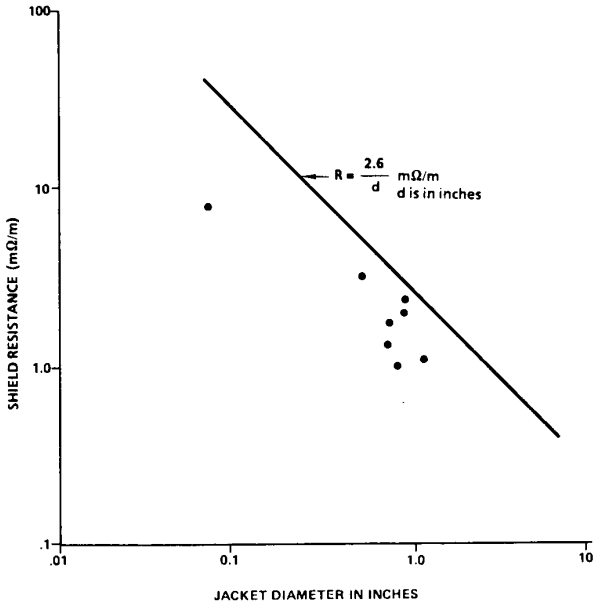

Fig. 30. Shield resistance as a function of cable diameter for double braid cables.

the shield. This can be predicted using (6). For a solid shield, the thickness and material determine the current diffusion break frequency and the high-frequency transfer impedance. For braided shields or those with apertures and other imperfections, the high-frequency surface transfer impedance is determined by the mutual inductance term, which can be due to both aperture and porpoising coupling. In most cases, porpoising coupling is dominant. However, many cables intentionally or unintentionally have come close to the optimum braid (in which case the aperture coupling is balanced against porpoising coupling). Note that the porpoising coupling depends on contact impedance and therefore is expected to change during the life of the cable.

In the preceding section, the surface resistance of a braided shield was found to be inversely proportional to the number of layers. In addition, each layer of braid reduces the mutual inductance by about a factor of ten. The following prediction models use this relatively simple theory to interpret the measured results from a large number of measurements [19].

Fig. 29 shows the shield resistance as a function of the braid diameter for single braid cables. Theory would suggest that the shield resistance should be inversely proportional to the diameter. This dependence is seen in Fig. 29. The solid straight line included in Fig. 29 is inversely proportional to the shield diameter and is an upper bound for the measured values. Fig. 30 shows the shield resistance as a function of cable diameter for double braid cables. Again, the $1/d$ dependence is clearly evident. Fig. 31 shows the measured shield mutual inductance as a function of cable diameter for single braid cables. At any particular diameter, the measurements are scattered over two orders of magnitude. Also shown in Fig. 31 are two lines that are inversely proportional to diameter or the square root of diameter. The line that is inversely proportional to the square root of the diameter provides an upper bound to

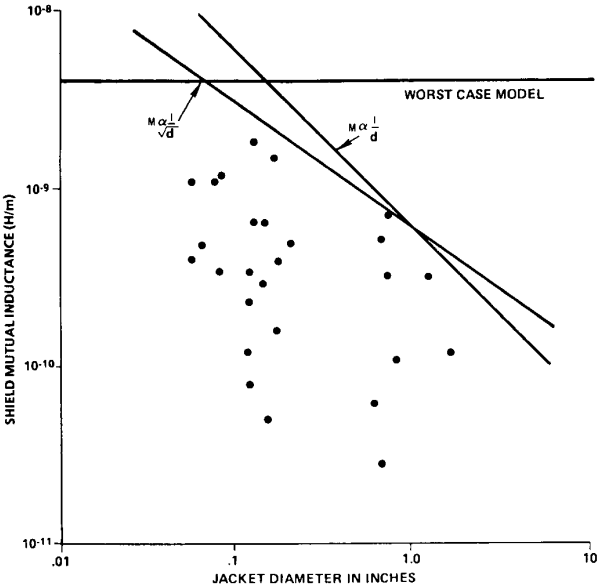

Fig. 31. Shield mutual inductance as a function of cable diameter for single braid cables.

the measured data. However, a theoretical basis cannot be given for such a dependence. Consequently, a worst case prediction model of 3×10^{-9} H/m for all cables, irrespective of diameter, is recommended. Fig. 32 shows the mutual inductance as a function of cable diameter for double braids. Although there are far fewer points in this figure, the scatter is again evident. The worst case model of 3×10^{-10} H/m chosen for the prediction model is based on the order of magnitude reduction in the mutual inductance that is usually seen when measuring one- and two-layer overbraids. For large cables,

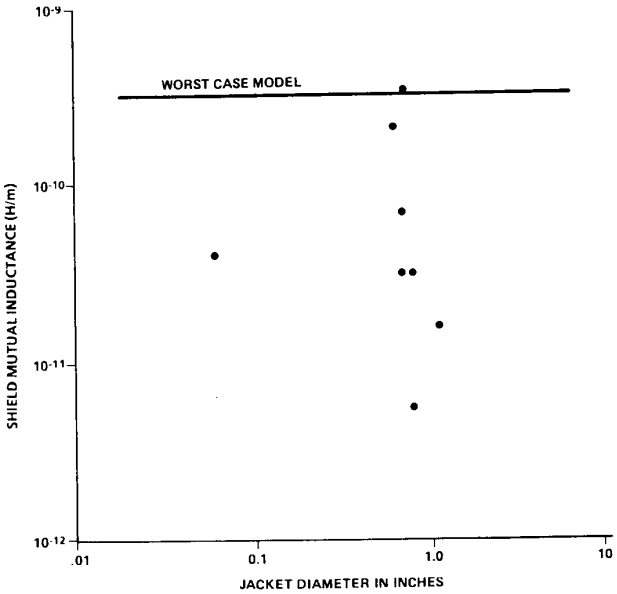

Fig. 32. Shield mutual inductance as a function of cable diameter for double braid cables.

TABLE I
WORST CASE LARGE BRAIDED CABLE MODEL

	R Ω/m	M H/m
SINGLE BRAID	4×10^{-3}	3×10^{-9}
DOUBLE BRAID	2×10^{-3}	3×10^{-10}
TRIPLE BRAID	1.5×10^{-3}	3×10^{-11}

namely those 25 mm (1 in) in diameter (plus or minus a factor of 2), a worst case model is presented in Table I.

Use of the prediction models presented in the preceding paragraphs should take into account some observations. The first of these is that optimum braids are probably more susceptible to degradation and should not be depended upon to maintain their performance throughout their lifetime. System survivability should be based on a worst case scenario as given in the cable model.

The second observation is that cables have a limited range of diameters. Shielded twisted pairs, coaxial transmission lines, etc., tend to have diameters that are within a factor of two of 1.25 mm (1/8 in). Large bundles are within a factor of two of a 25-mm (1-in) diameter. Consequently, simplified models can be developed using these two diameter ranges.

In the microwave region, the cable shield performance may depend on other parameters such as aperture coupling and small nonuniformly distributed holes. The prediction models presented in this section should be used cautiously in this frequency range.

If the worst case model were to be refined, the transfer resistance should be made inversely proportional to cable diameter. The mutual inductance is still best modeled as being independent of diameter. The transfer impedance of solid conduits can be predicted using the theory developed earlier in this paper.

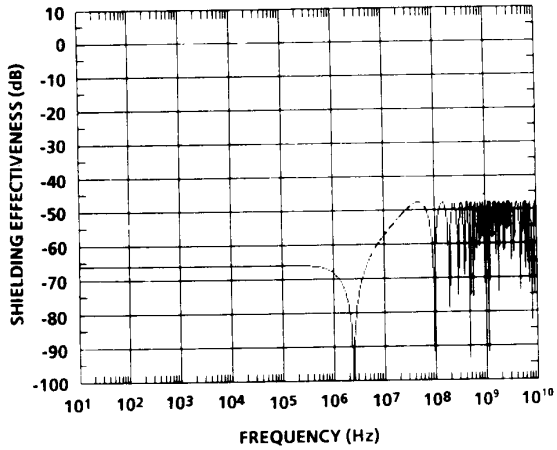

Fig. 33. Shielding effectiveness (ratio of currents) for a 1.2-m shielded twisted pair, calculated using surface transfer impedance.

VI. Calculation of Shielding Effectiveness

Irrespective of the problems alluded to earlier in this paper, a shielding effectiveness number is sometimes required to meet a specification. In some cases, this can be calculated from the surface transfer impedance and the geometry and impedances of the test set-up. A popular definition of shielding effectiveness (SEI) is the ratio (in decibels) of the current carried on the core to the current flowing on the shield. Reference [27] calculates shielding effectiveness according to this definition for the case of an electrically long cable that has a uniform distribution of imperfections such as the apertures in a braided shield. The theoretical treatment given in this reference assumes matched terminations and calculates a ratio of current shielding effectiveness. This reference shows that the shielding effectiveness can be written as (15).

$$SEI = 20 \log \frac{Z_T l}{2} + 20 \log \frac{\sin \theta}{\theta} - 10 \log (R_T)^2$$

$$\theta = \frac{\omega}{c} (\sqrt{\epsilon_r} + 1) \frac{l}{2} \tag{15}$$

where l is the length of the cable, R_T is the impedance used to terminate the center conductor, c is the velocity of light, and ϵ_r is the relative dielectric constant. At low frequencies, the shielding effectiveness depends on length, whereas at high frequencies, the mutual inductance coupling is limited by interference between multiple sources. The calculated shielding effectiveness of a shielded twisted pair is shown in Fig. 33. At low frequencies, the shielding effectiveness of this 1.2-m-long cable was about 70 dB, whereas at high frequencies, the shielding effectiveness decreased to only 48 dB. The surface transfer resistance and mutual inductance of the actual cable could be used to calculate the worst case values for the shielding effectiveness of such a cable.

VII. Conclusions

Schelkunoff showed that surface transfer impedance is the intrinsic property for describing electromagnetic shields. The transfer impedance measurement techniques are well established. Resistance measurements provide much of the desired information and are simple to make. Calibration samples establish the credibility of the measurement systems. Transfer impedance measurements are available on a variety of shields.

Acknowledgment

The authors wish to acknowledge the support of J. Gishpert of the Martin Marietta Strategic Systems Company, who helped direct much of the work reported here so that it addressed the challenging problems encountered in the design and installation of electromagnetically hardened systems and who encouraged the widespread publication of the results. The authors also wish to thank P. J. Madle for his enthusiastic encouragement and many stimulating discussions and suggestions. He freely shared the results of many years of work and much original thought. These were very valuable in planning and carrying out these measurements.

References

[1] P. J. Madle, "Cable and connector shielding attenuation and transfer impedance measurements using quadraxial and quintaxial test methods," in *Rec. IEEE Int. Symp. Electromagnet. Compat.*, 1975.

[2] S. A. Schelkunoff, "The electromagnetic theory of coaxial transmission lines and cylindrical shields," *Bell Syst. Tech. J.*, vol. 12, pp. 532–579, Oct. 1934.

[3] J. Zorzy and R. F. Muehlberger, "RF leakage characteristics of popular coaxial cables and connectors," *Microwave J.*, pp. 80–86, Nov. 1961.

[4] E. D. Knowles and L. W. Olsen, "Cable shielding effectiveness testing," *IEEE Trans. Electromagnet. Compat.*, vol. EMC-16, no. 1, pp. 16–23, Feb. 1974.

[5] E. F. Vance, "Shielding effectiveness of braided wire shields," *IEEE Trans. Electromagnet. Compat.*, vol. EMC-17, no. 2, pp. 71–77, May 1975.

[6] K. F. Casey and E. F. Vance, "EMP coupling through cable shields," *IEEE Trans. Electromagn. Compat.*, vol. EMC-20, no. 1, pp. 100–106, Feb. 1976.

[7] E. F. Vance, *Coupling to Shield Cables*. New York: Wiley Interscience, 1978, pp. 108–176.

[8] K. S. H. Lee and C. E. Baum, "Application of modal analysis to braided-shield cables," *IEEE Trans. Electromagn. Compat.*, vol. EMC-17, pp. 159–169, Aug. 1975.

[9] R. W. Latham, "Small holes in cable shields," *EMP Interaction Notes*, Note 118, Air Force Weapons Laboratory, Kirtland Air Force Base, NM, Sept. 1972.

[10] L. O. Hoeft and J. Hofstra, "A simple technique for measuring transfer admittance/capacitance," in *Rec. IEEE Int. Symp. Electromagn. Compat.*, pp. 835–837, Oct. 1984.

[11] E. P. Fowler, "Superscreened cables," *Radio Electron. Eng.*, vol. 49, no. 1, pp. 38–44, Jan. 1979.

[12] P. J. Madle, "Contract resistance and porpoising effects in braid shielded cables," in *Rec. IEEE Int. Symp. Electromagn. Compat.*, pp. 206–210, 1980.

[13] H. Kaden, *Wirbelstrome und Schirmung in der Nachrichtentechnic*. Berlin: Springer-Verlag, 1959.

[14] K. S. H. Lee, *EMP Interaction: Principles, Techniques, and Reference Data*. New York: Hemisphere, 1986.

[15] M. A. Dinallo, "Analysis concerning the effect of transfer admittance on transfer impedance measurements," in *Rec. IEEE Int. Symp. Electromagn. Compat.*, pp. 533–541, Aug. 1983.

[16] L. O. Hoeft, "Measurement of surface transfer impedance of cables and connectors," in *Rec. EMC-EXPO Int. Conf. Electromagn. Compat.* (Washington, DC), pp. T17.1–T17.15, June 1986.

[17] C. M. Hoeft, "Measured surface transfer impedance of ferromagnetic pipes and conduits," presented at NEM, Menlo Park, CA, May 1988.

[18] J. R. Hofstra, M. A. Dinallo, and L. O. Hoeft, "Measured transfer impedance of braid and convoluted shields," in *Rec. IEEE Electromagn. Compat. Symp.*, pp. 482–488, Sept. 1982.

[19] L. O. Hoeft, "A model for predicting the surface transfer impedance of braided cable," in *Rec. IEEE Int. Symp. Electromagn. Compat.*, pp. 402–404, Sept. 1986.

[20] L. O. Hoeft, J. Hofstra, and J. E. Merrell, "Measured transfer impedance of metallic and non-metallic conduits covered with tinned copper and SnCuFe braids," in *Rec. Int. Aerospace Ground Conf. Lightning Static Electricity*, pp. 44-1–44-7, June 1984.

[21] L. O. Hoeft and J. S. Hofstra, "Measured transfer impedance of metallized plastic tape and knitted wire mesh cable shields," in *Rec. IEEE Int. Symp. Electromagn. Compat.*, pp. 296–300, Aug. 1983.

[22] ——, "The effect of removing spring fingers and the wavy washer on the measured transfer impedance of a MIL-C-38999 series IV connector," in *Rec. IEEE Int. Symp. Electromagn. Compat.*, pp. 155–157, Sept. 1986.

[23] L. O. Hoeft, J. S. Hofstra, J. R. Evert, and J. E. Merrill, "Selected measurements of connectors, backshells, and cable terminations," *IEEE Trans. Nucl. Sci.*, vol. NS-33, no. 6, pp. 1688–1693, Dec. 1986.

[24] L. O. Hoeft and J. S. Hofstra, "Measured surface transfer impedance of various connector/backshell interfaces," in *Rec. 20th Annu. Connectors Interconnection Technology Symp.*, pp. 143–150, Oct. 1987.

[25] L. O. Hoeft, V. A. Gieri, and J. S. Hofstra, "Measured transfer impedance of a 11.5-inch diameter graphite epoxy composite tube with current diverters," in *Rec. IEEE Nat. Symp. Electromagn. Compat.*, pp. 35–38, Apr. 1984.

[26] J. S. Hofstra and L. O. Hoeft, "Measured transfer impedance and current reduction rations of a generic cableway," in *Rec. IEEE Int. Symp. Electromagn. Compat.*, pp. 521–525, Aug. 1983.

[27] M. Dinallo, L. O. Hoeft, and J. Hofstra, "Shielding effectiveness of typical cables from 1 MHz to 1000 MHz," in *Rec. IEEE Int. Symp. Electromagn. Compat.*, pp. 489–493, Sept. 1982.